ANNALS OF GEOPHYSICS, 69, 3, SY329, 2026; doi:10.4401/ag-9428
OPEN ACCESS

Discriminating the origin of obsidian fragments in archaeological contexts based on morphological features and geochemical data: the Breccia Museo (Campanian Ignimbrite eruption, Italy) case study

Bruna Cariddi[*,1], Franco Foresta Martin[2,3], Ilenia Arienzo[1], Lisetta Giacomelli[4], Paola Donato[5], Anna Russolillo[6,7], Sandro de Vita[1]

(1) Istituto Nazionale di Geofisica e Vulcanologia (INGV), Sezione Osservatorio Vesuviano, Naples, Italy
(2) Istituto Nazionale di Geofisica e Vulcanologia (INGV), Sezione di Palermo, Palermo, Italy
(3) Laboratorio Museo di Scienze della Terra, Ustica, Palermo, Italy
(4) Associazione Italiana di Vulcanologia, Italy
(5) Università della Calabria, DiBEST, Cosenza, Italy
(6) Università degli Studi Suor Orsola Benincasa di Napoli, Naples, Italy
(7) Associazione Villaggio Letterario, Ustica, Palermo, Italy

Article history: received September 18, 2025; accepted December 26, 2025

Abstract

A recent archaeological discovery on Vivara, the small islet next to Procida (Campania region, Italy), has documented the prehistoric use of finely crushed obsidian fragments as abrasive powder for polishing wooden artifacts. These fragments originated from a local deposit known as Breccia Museo – whose exploitation in prehistoric times had not been previously attested – and were found mixed with obsidian tools sourced from other well-known Italian deposits widely used throughout prehistory. To develop effective methods for discriminating obsidian provenance, as required in this case, we carried out geochemical, isotopic, and mineralogical analyses on obsidian samples collected from the Breccia Museo outcrop at Punta della Lingua (~4 km NE of Vivara), one of the richest and most accessible deposit on Procida Island. The results were compared with those obtained from Breccia Museo obsidians from other local (Campi Flegrei) outcrops, as well as with reference samples from the major obsidian sources exploited in the Central-Western Mediterranean during prehistory (Monte Arci, Palmarola, Lipari, and Pantelleria).

In addition, a micromorphological and microanalytical study was performed to identify further distinctive features useful for recognizing Breccia Museo obsidian across different archaeological contexts.

This interdisciplinary investigation highlights the potential of combining relatively rapid major/minor element analyses, mineralogical and morphological characterization, with more time-consuming but highly precise isotopic measurements ($^{87}Sr/^{86}Sr$, $^{143}Nd/^{144}Nd$) to achieve robust provenance discrimination.

Keywords: Breccia Museo Obsidians; Procida Island; Vivara Islet; Geochemical Fingerprint; Central-Western Mediterranean Obsidian Sources

1. Introduction

Mineralogical and petrographic techniques, together with analyses of chemical composition, have proven their soundness in determining the provenance of archaeological artifacts. Among the most common techniques used for this purpose are polarized light microscopy, Scanning Electron Microscope – Wavelength Dispersive X-ray Spectroscopy (SEM-WDS) analysis, X-ray Diffraction (XRD) for mineralogical analysis, X-ray Fluorescence (XRF) for major elements chemical analysis, and Laser Ablation for trace elements analysis.

Nevertheless, it is not always possible to discriminate the variable sources of raw materials (e.g., obsidians, ceramics, clays and temper) based on their chemical composition only, especially when sources producing such a material are similar in terms of major and trace elements contents. In this context, radiogenic isotopes analyses have been proven to represent a valuable tool for discriminating among the provenance of several categories of archaeological remains, such as lavas, clay and temper (e.g., De Bonis et al., 2018; Di Luzio et al., 2019). Similar approaches have been used in tephrochronology and in human mobility studies, by analyzing the chemical and isotopic composition of volcanic glass, sediments and human remains (Giaccio et al., 2017; Petrosino et al., 2019; Arienzo et al., 2020; D'Antonio et al., 2021; Pasquetti et al., 2023; Romboni et al., 2023).

The provenance of obsidian is one of the most important issues to be addressed in archaeological research. In prehistoric times, obsidian was a highly valued material, appreciated for its aesthetic appeal, sharpness, and ease of workability. It was widely used to produce extremely sharp blades, arrowheads, and scrapers, making it ideal for cutting, hunting, and skinning. In addition, some cultures employed obsidian to create mirrors, jewelry, and, on occasion, even for surgical procedures, due to its exceptional sharpness and precision (Scott and Scott, 1982; Disa et al., 1993; Chataigner et al., 1998; Tykot, 2021).

Obsidian has been described as "the black gold that came from the sea" (Foresta Martin and La Monica, 2019), as it was among the earliest materials to be widely traded. Numerous studies have demonstrated that obsidian was transported over hundreds of kilometers from its sources, suggesting the existence of complex exchange networks (e.g., Williams-Thorpe 1995; Tykot 2002, 2021). The study of its distribution provides valuable insights into early trade routes, interactions among ancient cultures, and the circulation of both materials and ideas.

The commercial trade of obsidian played a particularly significant role during the Neolithic period, especially in the Mediterranean region. In its central area, four main sources – Lipari, Pantelleria, Monte Arci and Palmarola – supplied large quantities of obsidian, that were exported to thousands of prehistoric settlements.

2. The Breccia Museo obsidian

Overlooking the waters of the Tyrrhenian Sea, deposits containing obsidian chunks and/or fragments mixed with tuff, ash, and variable type of lithic fragments, named Breccia Museo (BM hereafter), are found along the edge of the Campi Flegrei caldera west of Naples, within the city of Naples, along the coasts of Procida Island, and on the headland of Monte di Procida (Orsi et al., 1996; Fedele et al., 2008; Fig. 1a).

According to the latest radiometric dating and volcanological interpretations, these deposits share a common origin with the deposits of the Campanian Ignimbrite eruption, to which they are associated (e.g., Fedele et al., 2008). The Campanian Ignimbrite eruption is the largest volcanic event in the Mediterranean area, which dates to the Late Pleistocene (39.85 $\pm$ 0.14 ka BP; Giaccio et al., 2017).

Until recently, BM obsidians were believed to lack the structural properties necessary for knapping, and indeed, no artifacts attributable to this material had been discovered. However, recent archaeological excavation carried out on Vivara (Bertino et al., 2024), a satellite islet next to Procida (Fig. 1b), reports an unusual prehistoric use of obsidian attributed to the BM, easily collected from the deposits cropping out in several localities of the island. It should also be noted that in prehistoric times, sea level was several meters lower, and what is today known as the islet of Vivara, representing the remains of an ancient crater, was a strip of land firmly connected to the island of Procida (Marazzi and Tusa, 1994).

Procida's obsidian (Fig. 2) does not exhibit smooth or conchoidal black surfaces like that from Lipari, Palmarola, and Pantelleria, where it forms entire flows. Instead, it has a rough and granular surface, and is scattered as clasts among other volcanic materials of the BM. Nonetheless, its abundance, variety, and, perhaps not least, the fact that it is already reduced to fragments rather than large blocks to be quarried, may have driven the island's prehistoric inhabitants to use it in an era characterized by limited resources and a constant need for pointed and sharp tools.

Figure 1. (a) Structural sketch map of the Campi Flegrei Caldera west of Naples. Campi Flegrei is a nested caldera, formed by two main episodes of collapse, related to the Campanian Ignimbrite (ca. 40 ka BP) and the Neapolitan Yellow Tuff (ca. 15 ka BP) eruptions. After the latter eruption, volcanism concentrated within the youngest caldera (green dots in the figure). The Breccia Museo deposits are found along the caldera margins, within the city of Naples and on the facing island of Procida (Fedele et al., 2008). The caldera margins are simplified after Fedele et al. (2008); Trasatti et al. (2023); Sparice et al. (2024); (b) Location map of the sampled Breccia Museo outcrops in this study (red asterisk at Punta della Lingua) and in Fedele et al. (2008; purple asterisk at Scotto di Carlo), and main volcanic craters of the Procida activity (dashed black lines). Procida volcanoes are almost all older than the Campanian Ignimbrite eruption; only the Solchiaro volcano is dated between 19.6 and 15 ka (De Astis et al., 2004). Image data from Google Earth SIO, NOAA, U.S. Navy, NGA, GEBCO Landsat/Copernicus (14.12.2015-01.01.2021).

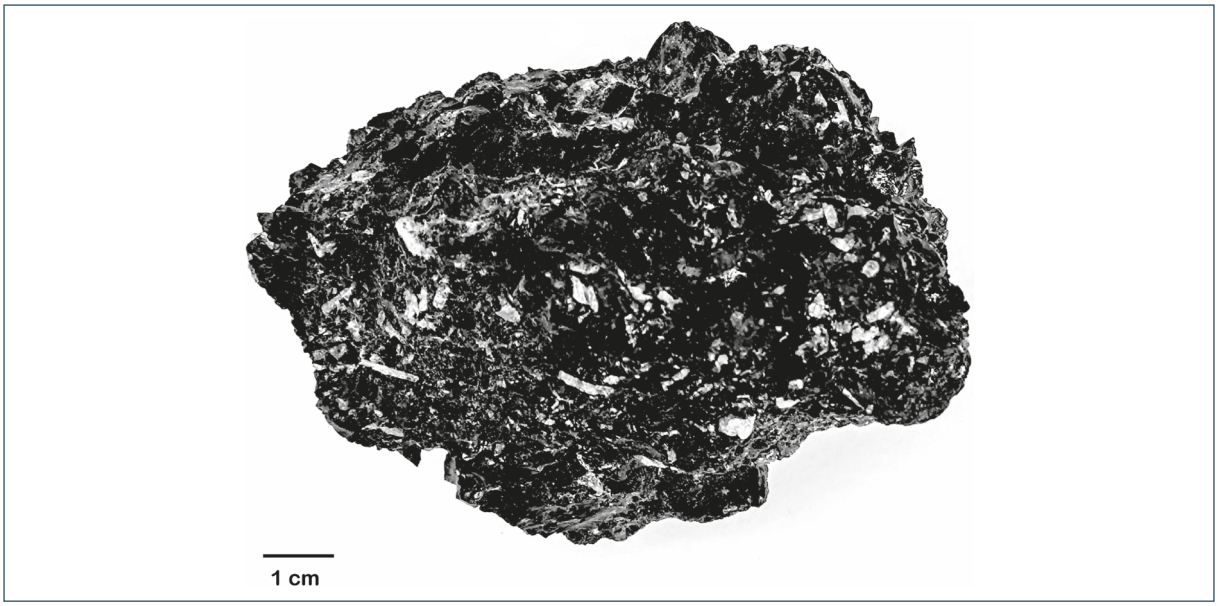

Figure 2. Obsidian chunk from BM deposit of Punta della Lingua, Procida. The granular surface stands out, characterized by the presence of abundant, macroscopic crystallites (photo by F. Foresta Martin).

To geochemically characterize the BM obsidian and establish a protocol to be used by archaeologists for discriminating among the different sources of obsidians in the Central-Western Mediterranean during prehistory, we performed the petrographic, morphologic and geochemical characterization of obsidian fragments. Our results testify that both major element geochemistry and isotope geochemistry are fundamental tools in geological and archaeological contexts, especially in contexts where raw materials, including obsidians, from multiple sources might be mixed.

2.1 Origin of the Breccia Museo

The BM term was coined at the end of the nineteenth century by the English geologist Henry James Johnston-Lavis to denote the heterogeneity of the deposit's constituents, its stratigraphic importance, and its peculiarity as an open-air museum showcasing a vast assortment of rock fragments from the Campi Flegrei (Johnston-Lavis, 1888; Fedele et al., 2008 and references therein). In current literature, this term is applied to both the lithic breccia deposit in the strict sense and the pyroclastic sequence in which these breccia deposits are included (Perrotta and Scarpati, 1994; Melluso et al., 1995; Rosi et al., 1996; Perrotta et al., 2006; Fedele et al., 2008). The lithic breccia is composed of a matrix-supported, heterogeneous deposit containing both fine and coarse particles, as well as rock fragments of different sizes and origins. Juvenile materials include ash, scoria, pumice, and dense glass like obsidian. Lithic materials encompass a wide variety of rocks, possibly broken off from the surrounding rocks during the ascent and fragmentation of magma. These materials include both fresh and altered lavas of different compositions, tuffs with variable degrees of alteration, loose crystals, and fragments of metamorphic and sedimentary rocks, all embedded within an ash-rich matrix. For our purposes, the term BM refer exclusively to the obsidian-bearing lithic breccia deposit.

The origin of the BM deposits has been a topic of debate for a long time, particularly regarding the location of the vent, the timing, and the sequence of events leading to their formation. Various studies on the subject have not always agreed. Some researchers have suggested that the deposits resulted from multiple small eruptions (Di Girolamo et al., 1984; Lirer et al., 1991), or from a roof collapse occurred during an explosive eruption ~20 ka ago (Perrotta and Scarpati, 1994; Melluso et al., 1995). The more widely accepted interpretation nowadays is that the BM deposits represent the proximal facies of the Campanian Ignimbrite eruption and originated from vents along the rim of the caldera created during the eruption (Rosi et al., 1996; Orsi et al., 1996; Pappalardo et al., 2002; Fulignati et al., 2004; Perrotta et al., 2006; Fedele et al., 2008) or erupted from vents located along regional faults partially reactivated during the caldera formation (Di Girolamo et al., 1984; Orsi et al., 1996).

The Campanian Ignimbrite is by far the product of the most powerful eruption to have occurred in the Mediterranean area, at least in the past 200 ka, with a bulk volume of tephra of 457-660 km^3 (181-265 km^3 Dense Rock Equivalent – DRE; Silleni et al., 2020), which corresponds to a mass of 4.7-6.9 $\times$ 10^{14} kg, (Magnitude M = 7.7-7.8; Pyle, 2015) and to a Volcanic Explosivity Index (VEI) of 7 (Cas et al., 2024). The eruption began with the development of a sustained Plinian-to-UltraPlinian eruptive column, which rose to a height of approximately 44 km (Rosi et al., 1999), resulting in a pumice-fall deposit that spread widely to the east. This Plinian phase was followed by the formation of Pyroclastic Density Currents (PDCs), which occurred as the eruption column collapsed, and the event transitioned into the ignimbritic phase. This phase was associated with the activation of multiple vents along fractures formed during the caldera collapse. The ignimbrites covered an area of 7,000 km^2 and flowed over ridges more than 1,000 m high (Barberi et al., 1978; Fisher et al., 1993). Ash fallout from both the Plinian and ignimbritic phases was dispersed extensively (Pyle et al., 2006), reaching as far East and North-East as the Don River in Siberia (Fedele et al., 2003).

As the BM deposits were observed resting above various pyroclastic flow units in different exposed areas (Perrotta and Scarpati, 1994; Perrotta et al., 2006), it can be suggested that the collapse did not happen simultaneously across the entire caldera region. However, it is believed to have occurred during a specific phase of the magma extraction phase of the eruption (Pappalardo et al., 2002; Perrotta et al., 2006). The latest $^{40}Ar/^{39}Ar$ radiometric analyses of samples from different BM outcrops (37.1 to 39.5 ka: Fedele et al., 2008) provide support for this interpretation by yielding an age that aligns with that of the main Campanian Ignimbrite deposit (39.85 $\pm$ 0.14 ka; Giaccio et al., 2017).

From a compositional point of view, pumice fragments from the Campanian Ignimbrite deposits show a chemical composition ranging from trachyte to trachy-phonolite (e.g., Civetta et al., 1997; Pappalardo et al., 2002; Fedele et al., 2008). The uppermost unit of the BM contains the least-evolved trachytic juvenile fragments, with a

CaO content of ~3.0-4.0 wt%. In contrast, the lowest units contain the most-evolved fragments (alkalitrachytic to phonolitic) with CaO ~1.5-2.0 wt% (Fedele et al., 2008). The different compositions were ascribed to different magmas feeding the eruption (e.g., Arienzo at al., 2009, 2011), featured by distinct Sr and Nd isotopic compositions (~0.70730 and ~0.70740; ~0.51247 and ~0.51250, respectively). PDCs associated with caldera collapse and juvenile materials from the BM unit exhibit chemical compositions that lie between the least- and most-evolved pumice samples (CaO = 1.9-2.9 wt%; Melluso et al., 1995; Pappalardo et al., 2002; Fedele et al., 2008).

2.2 Archaeological use of the BM obsidian

Recent archaeological studies on Vivara have revealed an unexpected prehistoric use of BM obsidian (Bertino et al., 2024 and references therein). This volcanic glass is unsuitable for producing typical cutting tools due to the abundance of microcrystals in its glassy matrix. In fact, BM obsidian breaks down into grains with even the slightest percussion, unlike obsidian from other sources in Italy, which were extensively used in prehistory for producing sharp blades and pointed tools. However, it has been established that the prehistoric communities of Vivara used it, not for making lithic tools, but as an abrasive for finishing the hulls of boats and other wooden artifacts (Bertino et al., 2024 and references therein).

This archaeological discovery has prompted us to undertake a study aimed at the geochemical characterization of obsidian fragments from the BM deposit of Punta della Lingua on Procida island. The obtained isotopic (Sr and Nd) and major oxides chemical compositions were compared with literature data on BM obsidians from Procida (Scotto di Carlo locality) and the inland Campi Flegrei area (Fedele et al., 2008) and with literature data on obsidians from Lipari, Palmarola, Monte Arci, and Pantelleria (Acquafredda and Paglionico, 2004; Francaviglia, 1988, 1999; Foresta Martin et al., 2017, 2020) in order to highlight the similarities and differences among different obsidian sources.

3. Materials and Methods

Our study is based on the analysis of obsidian samples from the BM collected on Punta della Lingua outcrop on Procida island (Fig. 1b) to determine: 1) morphology, petrography and composition of the mineral phases; 2) concentrations of major and minor elements; 3) Sr and Nd isotopic compositions.

Figure 3. The beach and promontory of Punta della Lingua in an aerial view from the north. BM obsidian deposits are found along the coastal cliff (Courtesy of Nicola Scotto di Carlo).

3.1 Description of Punta della Lingua outcrop and BM obsidian sampling

The obsidians from the BM analyzed in our research were collected at Punta della Lingua, a northeastern beach on the island of Procida (Fig. 3). It is the richest and most accessible obsidian outcrop on Procida, where the BM deposit reaches a maximum thickness of about 10 meters. It lies about 4 km from Vivara, which, when the islet was physically connected to Procida, could be traversed on foot.

Figure 4. (a) The BM deposit at Punta della Lingua, in Procida, where the sampling was carried out; (b) obsidian fragments at the foot of the BM outcrop at Punta della Lingua; (c) sharp-edged obsidian block embedded in the BM ash matrix; (d) obsidian block characterized by an external alteration patina; (e) obsidian fragments known as flames, embedded in a matrix of welded ash; (f) blocks of vesiculated pumice fragment with some obsidian crust (photos by Lisetta Giacomelli).

Numerous isolated obsidian fragments of variable sizes are scattered throughout the Punta della Lingua BM deposit (Fig. 4a) and are found in large numbers among the pebbles at the foot of the outcrop (Fig. 4b), produced by marine erosion cutting into the cliff's base.

Our sampling did not occur within a precise stratigraphic interval, given that the obsidian fragments are dispersed throughout the deposit, both as individual pieces and as inclusions in coarse breccia blocks and are prone to detachment from the deposit. Some of these fragments have a good degree of purity, possibly because they represent the parts most resistant to erosion and disintegration by the marine waves. For our geochemical, morphological and mineralogical analyses, we selected samples exhibiting greater compactness and low surface alteration, even if the external appearance tends to be granular due to the abundance of crystallites and vesicles (Fig. 2).

Although obsidian clasts represent a juvenile component of the BM deposit, the textural characteristics of the individual clasts are not homogeneous. In some cases, relatively pure, sharp-edged blocks of obsidian are found embedded in a matrix of welded ash (Fig. 4c). In other cases, obsidians are found in large blocks, coated with a grey or reddish patina resulting from chemical alteration, and the internal glassy structure is only revealed by breaking the block (Fig. 4d).

There are also obsidian fragments embedded in a matrix of welded ash, taking on forms known as "flames" (Fig. 4e), similar to those seen in many volcanic tuffs, such as the Campanian Ignimbrite "Piperno" facies (Rittmann, 1950). These structures, which are useful for understanding certain physical parameters of volcanic products, form in high-temperature ash and pumice flows. During transport and deposition, the still hot fragments of pumice can be deformed until their characteristic porosity is completely erased, transforming into flattened structures of translucent glass. Some vesiculated pyroclastic rock blocks have lost porosity in their external areas, resulting in the formation of an obsidian crust (Fig. 4f).

3.2 Micro-morphological and geochemical analyses of the BM obsidian

Different types of analyses were performed on selected fragments of obsidian from the BM deposit of Punta della Lingua (Procida):

- *Micro-morphological observation and microanalysis* were performed on three small fragments of BM obsidian (Fig. 5) at the Center for Microscopy and Microanalysis of the Department of Biology, Ecology and Earth Sciences at the University of Calabria, by using a Zeiss Crossbeam 350 Ultra High Resolution Scanning Electron Microscope (SEM) equipped with an EDAX Octane Elite Plus Energy Dispersion Spectrometer (EDS). Both the natural surface of the obsidian and the artificially cut, polished surfaces, were observed in Secondary Electrons (SE) and Back-Scattered Electrons (BSE). The microanalyses were performed on the polished section of each sample under the following conditions: working distance of 13 mm, HV of 15 keV, probe current of 100 nA, take-off angle of 40° and acquisition live time of 60 sec. Results of analyses are in Tables 1 and 2.
- *Chemical analyses* were conducted at the High Pressure-High Temperature Laboratory of the Istituto Nazionale di Geofisica e Vulcanologia (INGV) in Rome, to determine the chemical composition of major and minor elements

Figure 5. Three obsidian fragments already cut, polished and carbon-coated, ready for morphological and mineralogical analysis under the electron microscope (photo by Paola Donato).

in the obsidian, adopting the following standards: albite (Si, Al, Na), forsterite (Mg), augite (Fe), rutile (Ti), orthoclase (K), apatite (P, Ca), sodalite (Cl) and rhodonite (Mn). The analyses were performed by using a JEOL-JXA-8200 electron microprobe equipped with an energy-dispersive (EDS) X-ray spectrometer and five wave-length dispersive (WDS) X-ray spectrometers. The results are reported in Table 3.

– *Sr and Nd isotopic compositions* of selected obsidian fragments from Punta della Lingua BM, Lipari, Palmarola, Monte Arci and Pantelleria, were determined by Thermal Ionization Mass Spectrometry at the Radiogenic Isotope Laboratory (RIL) of the INGV, Osservatorio Vesuviano, following samples dissolution and Sr and Nd extraction by chromatographic techniques on columns (Arienzo et al., 2013). Determinations of $^{87}Sr/^{86}Sr$ and $^{143}Nd/^{144}Nd$ were performed by using a Thermo Scientific™ Triton™ Plus mass spectrometer (Cariddi et al., 2025). Measured Sr and Nd isotopic ratios were normalized for within-run isotopic fractionation to $^{86}Sr/^{88}Sr = 0.1194$ and $^{146}Nd/^{144}Nd = 0.7219$, respectively. For each single measurement, with N = 175, the standard error (2SE) was better than ±0.000007 for Sr, and better than ±0.000008 for Nd. During the period of analysis, the mean measured value of $^{87}Sr/^{86}Sr$ for the NIST-SRM 987 international standard was 0.710242 ± 0.000013 (2σ, N = 58); the mean measured value of $^{143}Nd/^{144}Nd$ for the JNdi-1 international standard was 0.512103 ± 0.000007 (2σ, N = 34); the external reproducibility (2σ) during the period of measurements was calculated according to Goldstein et al. (2003). The measured Sr and Nd isotope ratios were finally normalized to the recommended value of the standards: 0.710248 for Sr and 0.512107 for Nd (Zhang and Hu, 2020). Results of analyses are in Table 4.

4. Results and Discussions

4.1 Morphology, mineralogy and phase composition of the BM obsidian from Punta della Lingua

The most evident characteristic of all three BM fragments analyzed in this study is the occurrence, on the natural surface, of numerous vesicles, mostly rounded in shape and varying in size from a few dozens to a few hundred micrometers. On the same natural surface, it is also possible to observe several hydration cracks (Fig. 6a). Observation of the fresh cut confirmed the presence of vesicles with a variable shape depending on the orientation of the cut. Vesicles appear randomly distributed and arranged in the cuts in which they appear rounded. However, on artificial surfaces where elongation is accentuated, they often appear with the major axis iso-oriented and arranged in preferential alignments (Fig. 6b). The groundmass of the obsidian fragments is entirely glassy. However, several phenocrysts and microphenocrysts can be observed (Fig. 7), with dimensions ranging from few tens of micrometers to more than one millimeter.

Clinopyroxene is one of the most common mineral phases, typically occurring as idiomorphic crystals with dimensions exceeding half a millimeter (Fig. 7a). Its composition falls in the field of diopside (Fig. 8a; Table 1).

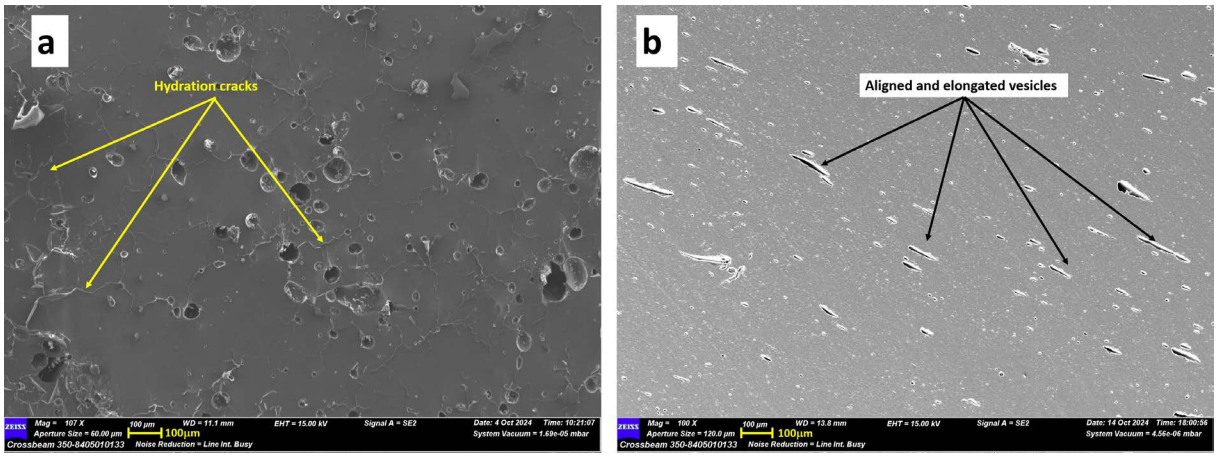

Figure 6. (a) SE-SEM image of the natural surface of obsidians from Punta della Lingua (Procida), on which rounded vesicles and hydration cracks are visible; (b) SE-SEM image of the artificially cut, polished surface, showing the occurrence of several elongated and iso-oriented vesicles. The length of the yellow scale bar corresponds to 100 micrometers (photos by Paola Donato).

Zoned crystals have been frequently observed, with magnesium-rich cores and rims richer in iron (Figs. 7a and b, Fig. 8a; Table 1).

The sialic phases are mainly represented by alkali feldspar and, subordinately, by plagioclase. The alkali feldspar crystals can be classified as anorthoclase and sanidine (Fig. 8b). They reach dimensions of even several millimeters,

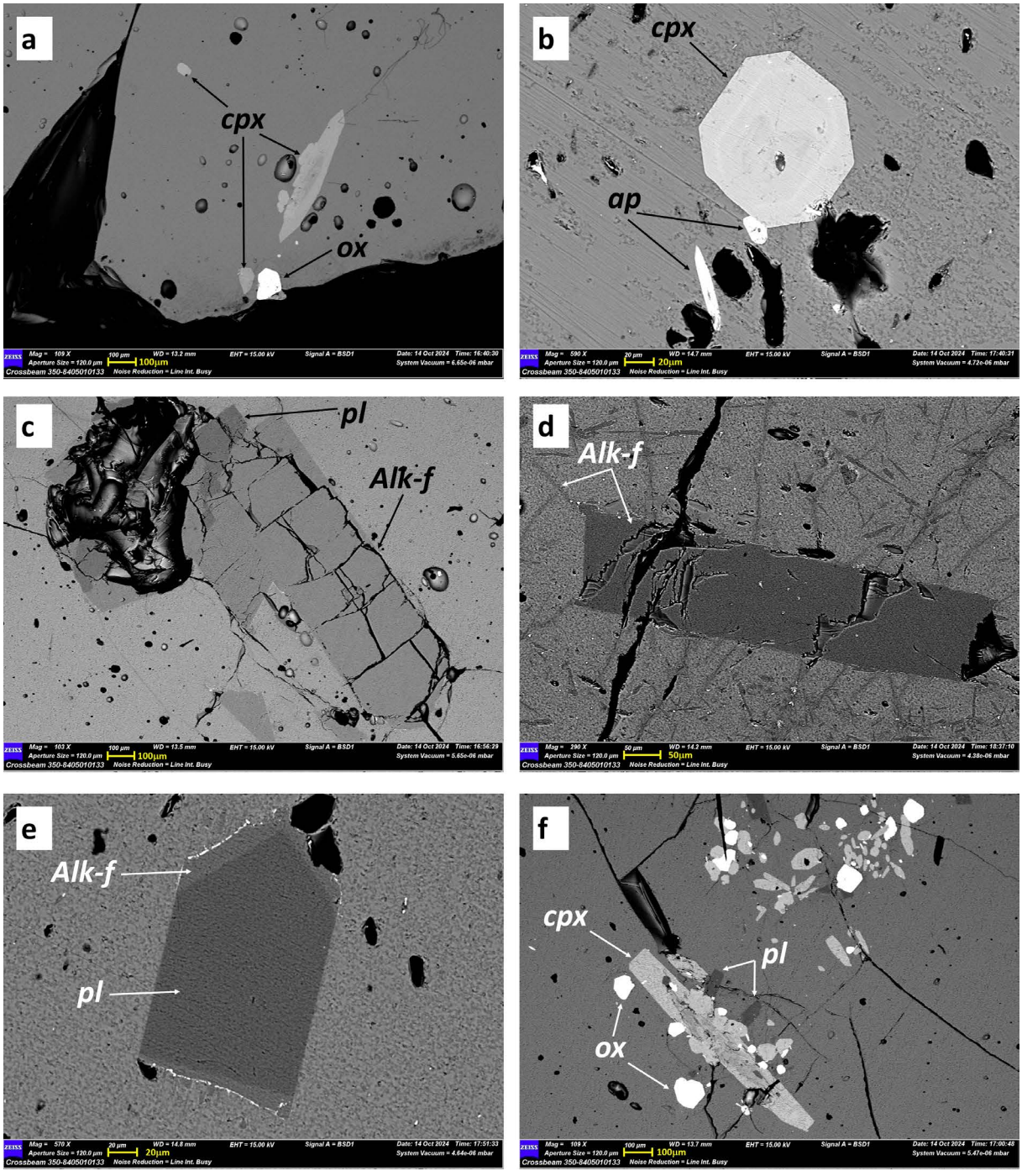

Figure 7. (a) Phenocryst of zoned clinopyroxene (cpx), corresponding to analyses BM1_19 in Table 1, smaller clinopyroxenes and a Fe-Ti oxide (ox) are also visible, the yellow scale bar is 100 micrometers; (b) zoned clinopyroxene with two small apatites (ap), scale bar: 20 micrometers; (c) fractured phenocryst of alkali-feldspar (alk-f) with a smaller plagioclase (pl), scale bar: 100 micrometers; (d) phenocryst and acicular microphenocrysts of alkali-feldspar; scale bar: 50 micrometers. (e) plagioclase surrounded by a rim of alkali-feldspar, corresponding to analyses BM2_13 in Table 2, scale bar: 20 micrometers; (f) pseudo-cumulite of clinopyroxene (a zoned crystal is well visible), Fe-Ti oxides and plagioclases, with the same minerals at the top of the image, scale bar: 100 micrometers. All the images have been acquired in BSE (photos by Paola Donato).

Table 1. Composition of pyroxene, apatite and oxides. Cpx: clinopyroxene; mph: microphenocryst; ph: phenocryst.

Pyroxene								
Sample	**BM1 17**	**BM1 19**		**BM1 30d**	**BM2 01bis**	**BM2 12bis**	**BM2 30**	**BM2 30b**
type	cpx mph core	cpx ph core	cpx ph rim	cpx ph core	cpx mph core	cpx mph core	cpx mph core	cpx mph core
SiO_2 (wt%)	52.3	47.9	47.5	49.1	53.3	53.6	53.3	53.0
TiO_2	0.0	1.5	1.2	1.0	0.0	0.2	0.0	0.0
Al_2O_3	2.8	5.8	4.3	3.6	2.9	3.5	2.8	3.6
Fe_2O_3	1.9	9.6	12.0	8.3	0.0	0.0	0.0	0.0
FeO	8.1	0.0	0.0	2.2	8.7	8.3	8.7	8.9
MnO	0.7	0.0	1.1	0.8	0.5	0.5	0.6	0.5
MgO	12.3	15.0	11.8	11.9	13.2	13.1	12.9	12.9
CaO	21.1	22.1	21.3	22.3	20.4	19.7	20.7	20.1
Na_2O	0.9	0.9	1.5	1.2	1.0	1.2	1.0	1.0
K_2O	0.2	0.5	0.5	0.4	0.0	0.0	0.0	0.0
En	36.9	43.4	34.9	35.2	40.0	40.7	39.1	39.5
Fe	17.7	10.6	19.8	17.4	15.6	15.3	15.8	16.2
Wo	45.5	46.0	45.3	47.4	44.4	44.0	45.1	44.3
Mg#	0.7	0.8	0.6	0.7	0.7	0.7	0.7	0.7

Apatite		
Sample	**BM2 12**	**BM2 31**
type	ap ph core	ap ph core
SiO_2 (wt%)	2.1	2.5
Al_2O_3	0.3	0.5
P_2O_5	34.4	34.4
CaO	54	51.6
Na_2O	0	0.3
K_2O	0.2	0
F	3.3	4.2
Cl	0.3	0.3
Y_2O_3	3.3	3.6
Cs_2O	0.1	0
Ce_2O_3	1.2	1.3
Nd_2O_3	0.7	1.2

Oxides					
Sample	**BM1 19c**	**BM1 30a**	**BM1 30c**	**BM1 36**	**BM1 37**
type	ph core	ph core	ph core	mph core	mph core
SiO_2 (wt%)	0.7	0.5	1.7	0.6	0.5
TiO_2	9.8	9.9	9.6	10	9.6
Al_2O_3	2.4	2.2	3	2.6	2.5
FeO	83.3	84.1	80.1	83	83.1
MnO	1.7	1.9	1.7	1.6	1.8
MgO	2	1.4	2.2	2.3	2.5
Na_2O	0	0	1.6	0	0

are often fractured and associated with smaller plagioclase crystals (Fig. 7c). In some cases, the alkali feldspar also occurs as acicular micro-phenocrysts, sometimes associated with larger crystals (Fig. 7d). In a few cases, an alkali feldspar rim is observed around a plagioclase crystal (Fig. 7e, Fig. 8b; Table 2). Plagioclases are generally smaller and less abundant than alkali-feldspars and can be classified as oligoclase with a few terms slightly Ca-richer falling in the field of andesine (Fig. 8; Table 2).

Among the accessory phases, iron and titanium oxides are very common (Table 1), with dimensions even larger than 100 micrometers. Apatite generally occurs as small crystals with dimensions in the order of some dozens of micrometers and is characterized by the occurrence of moderate amounts of fluorine, chlorine and Rare Earths Elements (Table 1). The different mineral phases are sometimes associated to form clusters or pseudo-cumulites (Fig. 7f).

The distinctive features of vesicularity and crystallinity allow the BM obsidians to be distinguished from those of other Italian sources, even in absence of chemical analysis by electron microprobe or XRF. The obsidians from Lipari are completely devoid of vesicles and aphyric (Donato et al., 2018), or, at most, contain rare microphenocrysts of pyroxene (Acquafredda and Paglionico, 2004). Similarly, the obsidians from Palmarola contain only sparse microcrystals of pyroxene (Acquafredda and Paglionico, 2004), whereas those from Pantelleria are characterized by the presence of feldspars together with crystals of aegirine-augite, amphibole, and aenigmatite (Rotolo et al., 2020). Finally, the obsidians from Monte Arci, which are the most crystalline among the Italian sources, contain abundant microcrystals of feldspar and biotite, along with rare clinopyroxene (Acquafredda and Paglionico, 2004). The presence of micro vesicles has never been reported in the obsidians from any of the Italian sources.

Table 2. Composition of feldspars. Pl: plagioclase; Alk-f: Alkali-feldspar; mph: microphenocryst; ph: phenocryst.

Feldspar															
Sample	**BM1 25c**	**BM1 33**	**BM1 34**	**BM1 35**	**BM1 38b**	**BM2 01**	**BM2 11**	**BM2 11c**	**BM2 11d**	**BM2 13**		**BM2 14**		**BM3 30**	**BM3 31**
type	Pl mph core	Pl ph core	Pl mph core	Pl mph core	Pl ph rim	Alk-f mph core	Alk-f ph core	Alk-f ph core	Alk-f mph core	Pl mph core	Alk-f mph rim	Pl mph core	Alk-f mph rim	Alk-f mph core	Alk-f mph core
SiO_2 (wt%)	59.3	58.7	58.4	58.9	59.4	64.2	64.4	63.9	64.5	60.0	64.1	60.1	63.8	63.2	63.6
Al_2O_3	25.2	25.4	24.9	24.7	25.1	20.5	20.5	20.2	20.4	24.9	21.0	25.0	21.2	21.0	20.2
Fe_2O_3	0.0	0.0	1.0	0.7	0.0	0.0	0.0	0.0	0.0	0.0	1.1	0.0	1.0	1.2	0.0
CaO	5.5	5.7	5.5	5.0	5.0	1.1	0.9	0.9	1.0	5.7	1.7	5.4	1.8	2.0	1.0
Na_2O	8.1	8.4	8.4	8.6	8.8	4.4	4.4	4.6	4.4	7.2	5.5	7.5	5.6	7.1	5.4
K_2O	1.9	1.8	1.8	2.1	1.8	9.8	9.7	10.0	9.8	2.1	6.7	2.1	6.7	5.6	9.3
Ab	65.4	66.0	66.5	67.5	69.0	38.4	39.0	39.4	38.6	61.4	50.7	63.2	50.9	59.7	44.7
An	24.5	24.7	24.1	21.7	21.7	5.3	4.4	4.3	4.8	26.8	8.7	25.1	9.0	9.3	4.6
Or	10.1	9.3	9.4	10.8	9.3	56.3	56.6	56.3	56.6	11.8	40.6	11.6	40.1	31.0	50.7

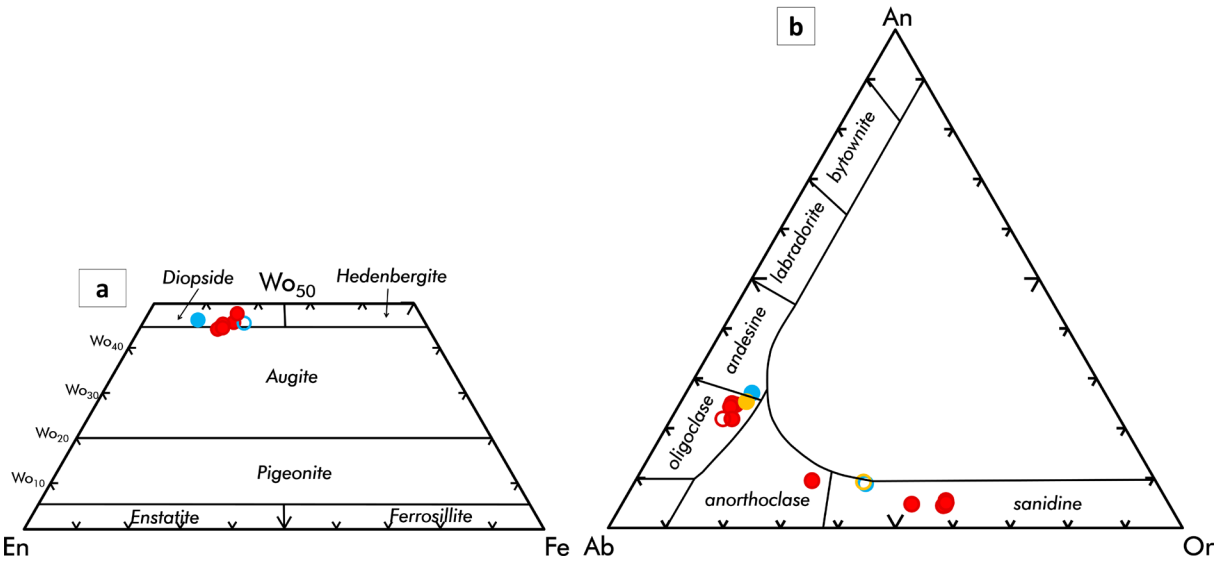

Figure 8. Classification diagrams for (a) pyroxenes and (b) feldspars of the obsidians from Punta della Lingua (Procida). Solid and empty symbols of the same color indicate, respectively, the core and rim of the same crystal.

4.2 Major elements geochemistry of the BM obsidian from Punta della Lingua

Following the TAS [Total Alcali ($Na_2O + K_2O$) vs. Silica (SiO_2), (Le Bas et al., 1986)] classification diagram of igneous rocks, the BM obsidian from Punta della Lingua deposit, analyzed in this study, is a trachy-phonolite. Its major oxides element composition (SiO_2 = 61.4 wt%, Al_2O_3 = 19.0 wt%, Fe_2O_{3T} = 3.3 wt%, MgO = 0.4 wt%, CaO = 1.6 wt%, Na_2O = 6.6 wt%, K_2O = 7.1 wt%; Table 3) closely overlaps with that of the BM obsidians from the Scotto di Carlo (Fig. 1b) deposit on Procida Island (Fedele et al., 2008), which fall in the wider compositional range of the BM obsidians from inland deposits (e.g., MgO = 0.2-1.7 wt%, Fedele et al., 2008; Fig. 9).

In the TAS diagram (Fig. 9a), all the BM obsidians are clearly distinguishable from the four most commonly used Central-Western Mediterranean sources of obsidians, i.e. Lipari and Pantelleria (Sicily), Monte Arci (Sardinia), and Palmarola (Pontine Archipelago, Latium), due to the lower silica (~59-62 wt%), and higher alkalis contents (~12-14 wt%). Indeed, these latter are predominantly rhyolites, with SiO_2 >69 wt%, differing from the trachy-phonolites of BM. The Italian obsidian sources, which supplied thousands of prehistoric villages in the Central-Western Mediterranean area with raw materials, form two groups in the TAS diagram (Fig. 9a): Lipari, Monte Arci and Palmarola are characterized by high silica content (72.6-76.8 wt%) and generally low alkali contents (8.3-10.5 wt%), whereas Pantelleria, more detached, exhibits lower silica (<73 wt%) and higher alkali contents (~11 wt%). However, some samples collected in the northern sector of Pantelleria straddle in the trachyte field, with even lower silica (~66-68 wt%) and slightly higher alkalis (~11.5 wt%) contents.

When other major elements such as Al_2O_3 and Fe_2O_{3T}, are considered (Figs. 9b and c), the distinctive chemical signature of the BM obsidians is still evident. They exhibit the highest Al_2O_3 contents (~18-19 wt%), and intermediate Fe_2O_{3T} values (~3-4 wt%). In comparison, Pantelleria obsidians show the highest Fe_2O_{3T} concentrations (~6-10 wt%) and the lowest Al_2O_3 values (~8-11 wt%), whilst obsidians from Lipari, Palmarola, and Monte Arci are grouped together by their low Fe_2O_{3T} content (~0-2 wt%) and intermediate Al_2O_3 values (~13-14 wt%). This chemical distinction further supports the separation of Pantelleria and BM obsidians from other Central-Western Mediterranean sources.

Given the significant compositional overlap among Lipari, Monte Arci, and Palmarola obsidians, both in the TAS diagram (Fig. 9a) and in major oxides variation diagrams (Figs. 9b and c), further geochemical discriminators are necessary to reliably distinguish between them.

Some authors (e.g., Williams-Thorpe, 1995) have found that the Shand's diagram (Shand, 1927), which is used to estimate the proportions of alumina, alkali and calcium through the two Alumina Saturation Index (ASI = molar ratio of $Al_2O_3/(CaO + Na_2O + K_2O)$), and Agpaitic Index (AI = molar ratio of $Al_2O_3/(Na_2O + K_2O)$), can be useful to discriminate the obsidian sources. The obsidians from Pantelleria are clearly distinguishable due to their

Table 3. Measured major elements and chlorine concentration in fragments of the Breccia Museo obsidians sampled in Punta della Lingua outcrop (Procida). The analyses have been recalculated to 100 wt% without volatile elements, considering Fe_2O_{3T} (calculated as $FeO_T/0.8998$). The mean values, plotted in the diagrams, of the 20 analyses carried out on the different fragments, are reported in bold. $AI = Al/(Na + K) = (Al_2O_3 * 2/101.96)/\big((Na_2O * 2/61.98) + (K_2O * 2/94.196)\big)$;
$ASI = Al/(Ca + Na + K) = (Al_2O_3 * 2/101.96)/\big((CaO/56.08) + (Na_2O * 2/61.98) + (K_2O * 2/94.196)\big)$.

Sample	Procida 1_Breccia Museo																				Procida1
Fragment	a	a	b	b	c	c	d	d	e	e	d	d	f	f	g	g	h	i	l	m	**Mean**
SiO_2 (wt%)	60.42	59.98	60.08	59.91	59.98	60.18	61.07	60.87	60.81	61.02	60.04	60.65	60.68	60.88	61.09	60.69	60.07	60.00	60.70	60.67	**60.49**
TiO_2	0.51	0.13	0.55	0.70	0.34	0.40	0.60	0.26	0.85	0.47	0.64	0.43	0.45	0.13	0.21	0.34	0.51	0.62	0.45	0.19	**0.44**
Al_2O_3	18.59	18.57	18.84	18.70	18.72	18.58	18.89	18.82	18.81	18.94	18.53	18.92	18.82	19.10	18.87	18.56	18.60	18.43	19.06	18.58	**18.75**
FeO_T	2.91	3.07	2.89	2.96	2.86	2.90	3.01	3.03	3.02	2.80	2.77	2.86	2.78	2.87	3.05	3.04	2.86	2.90	2.93	2.83	**2.92**
MnO	0.26	0.27	0.31	0.33	0.22	0.19	0.19	0.17	0.26	0.13	0.20	0.20	0.20	0.25	0.26	0.27	0.17	0.18	0.22	0.21	**0.23**
MgO	0.38	0.32	0.40	0.39	0.32	0.34	0.37	0.42	0.39	0.44	0.37	0.40	0.42	0.43	0.42	0.35	0.37	0.41	0.32	0.34	**0.38**
CaO	1.61	1.51	1.56	1.75	1.36	1.70	1.62	1.52	1.83	1.63	1.51	1.83	1.38	1.55	1.44	1.61	1.58	1.49	1.44	1.65	**1.58**
Na_2O	6.53	6.32	6.53	6.54	6.44	6.37	6.65	6.45	6.42	6.52	6.66	6.52	6.54	6.41	6.33	6.44	6.41	6.41	6.38	6.39	**6.46**
K_2O	7.16	7.10	7.12	6.99	6.85	7.00	6.40	6.87	7.00	7.37	6.78	7.02	7.00	6.80	6.52	6.74	7.20	7.07	6.71	7.27	**6.95**
P_2O_5	0.07	0.11	0.02	0.02	0.03	0.09	0.01	0.10		0.07	0.04	0.08	0.09	0.07	0.02	0.03		0.01	0.03	0.07	**0.05**
Total	98.44	97.38	98.30	98.30	97.13	97.75	98.81	98.50	99.39	99.40	97.54	98.90	98.36	98.49	98.22	98.07	97.77	97.53	98.24	98.20	**98.24**
Cl	0.71	0.73	0.72	0.63	0.73	0.72	0.76	0.68	0.69	0.69	0.81	0.74	0.68	0.76	0.74	0.69	0.72	0.68	0.67	0.69	**0.71**
Fe_2O_{3T}	3.23	3.41	3.21	3.29	3.18	3.22	3.35	3.37	3.36	3.11	3.08	3.18	3.09	3.19	3.39	3.38	3.18	3.22	3.26	3.15	**3.24**
Recalculated to 100 wt%																					
SiO_2	61.18	61.38	60.92	60.74	61.55	61.36	61.60	61.59	60.98	61.20	61.36	61.13	61.50	61.61	61.98	61.67	61.24	61.32	61.58	61.58	**61.37**
TiO_2	0.52	0.13	0.56	0.71	0.35	0.41	0.60	0.26	0.85	0.47	0.65	0.43	0.45	0.13	0.22	0.35	0.52	0.63	0.46	0.19	**0.44**
Al_2O_3	18.82	19.00	19.10	18.96	19.21	18.95	19.05	19.04	18.86	19.00	18.94	19.07	19.07	19.33	19.15	18.86	18.96	18.83	19.34	18.86	**19.02**
Fe_2O_{3T}	3.27	3.49	3.26	3.34	3.26	3.29	3.37	3.41	3.37	3.12	3.15	3.20	3.13	3.23	3.44	3.43	3.24	3.29	3.30	3.19	**3.29**
MnO	0.27	0.28	0.31	0.34	0.23	0.19	0.19	0.17	0.26	0.13	0.21	0.20	0.20	0.26	0.27	0.27	0.17	0.19	0.23	0.21	**0.23**
MgO	0.38	0.33	0.40	0.40	0.33	0.34	0.38	0.42	0.39	0.45	0.38	0.40	0.43	0.44	0.43	0.36	0.38	0.42	0.32	0.35	**0.39**
CaO	1.63	1.55	1.58	1.77	1.39	1.73	1.63	1.54	1.84	1.63	1.54	1.84	1.40	1.57	1.46	1.64	1.61	1.52	1.46	1.67	**1.60**
Na_2O	6.61	6.47	6.62	6.63	6.61	6.50	6.71	6.53	6.44	6.54	6.81	6.57	6.63	6.49	6.42	6.54	6.53	6.55	6.47	6.49	**6.56**
K_2O	7.25	7.27	7.22	7.09	7.03	7.14	6.46	6.95	7.02	7.39	6.93	7.08	7.09	6.88	6.62	6.85	7.34	7.23	6.81	7.38	**7.05**
P_2O_5	0.07	0.11	0.02	0.02	0.03	0.09	0.01	0.10	0.00	0.07	0.04	0.08	0.09	0.07	0.02	0.03	0.00	0.01	0.03	0.07	**0.05**
Total	**100.0**	**100.0**	**100.0**	**100.0**	**100.0**	**100.0**	**100.0**	**100.0**	**100.0**	**100.0**	**100.0**	**100.0**	**100.0**	**100.0**	**100.0**	**100.0**	**100.0**	**100.0**	**100.0**	**100.0**	**100.0**
Na_2O+K_2O	13.86	13.73	13.84	13.72	13.64	13.63	13.16	13.48	13.46	13.93	13.74	13.65	13.72	13.37	13.04	13.39	13.88	13.78	13.28	13.87	**13.61**
Al/(Na+K)	1.01	1.03	1.02	1.02	1.04	1.03	1.06	1.04	1.04	1.01	1.01	1.03	1.03	1.07	1.08	1.04	1.01	1.01	1.07	1.01	**1.03**
Al/(Ca+Na+K)	0.93	0.95	0.95	0.94	0.97	0.95	0.98	0.97	0.95	0.94	0.94	0.95	0.96	0.99	1.00	0.96	0.94	0.94	1.00	0.93	**0.96**
$SiO_2/(Na_2O+K_2O)$	4.41	4.47	4.40	4.43	4.51	4.50	4.68	4.57	4.53	4.39	4.47	4.48	4.48	4.61	4.75	4.60	4.41	4.45	4.64	4.44	**4.51**

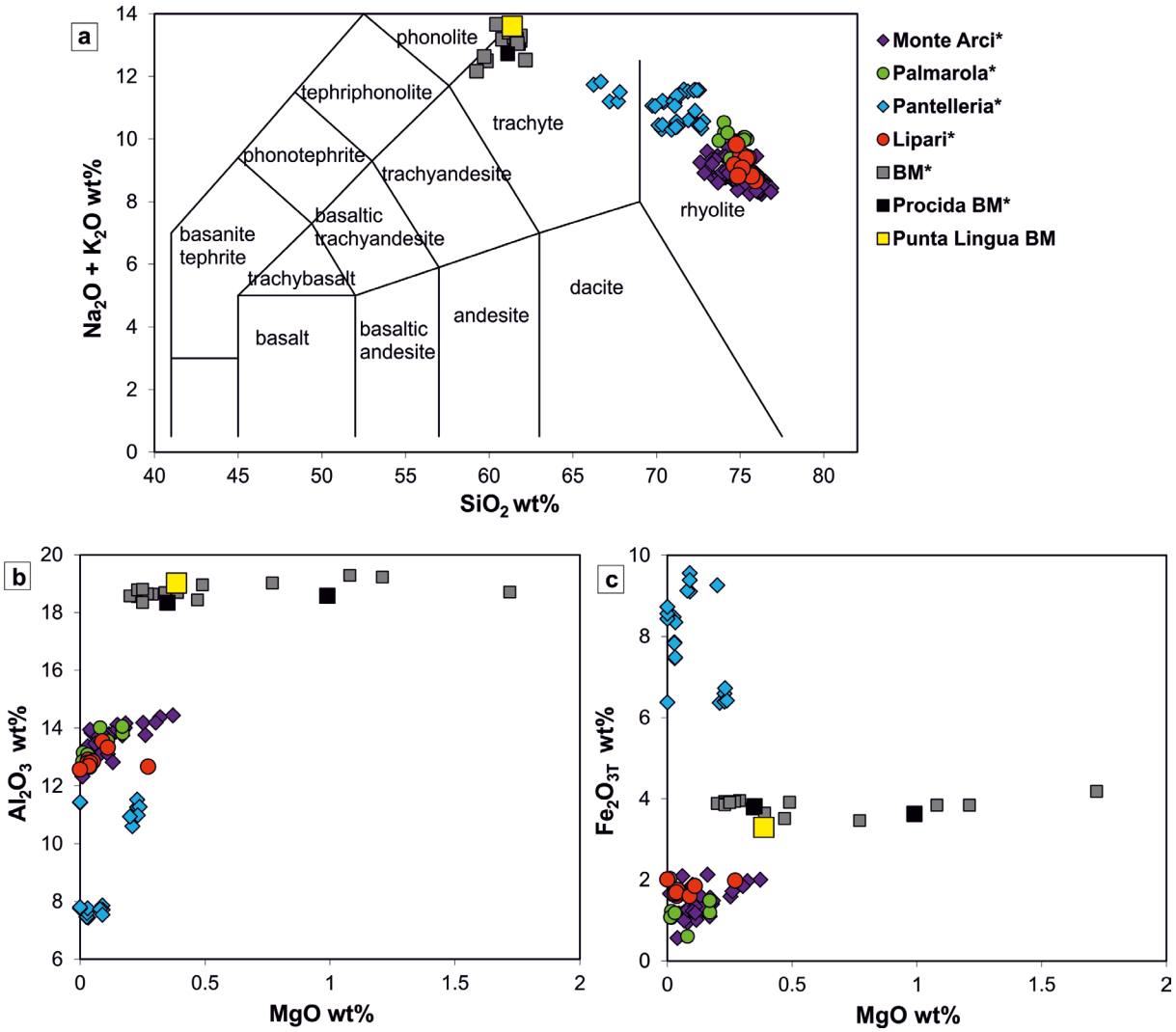

Figure 9. (a) TAS classification diagram (Le Bas et al., 1986), (b) MgO (wt%) vs. Al_2O_3 (wt%) and (c) MgO (wt%) vs. Fe_2O_{3T} (wt%) diagrams showing Punta della Lingua BM obsidian analyzed in this study, compared with literature data of obsidians from Monte Arci*, Palmarola*, Pantelleria*, Lipari* (Francaviglia, 1984, 1988, 1999; Tykot, 2002; Gioncada et al., 2003; Bellot-Gurlet et al., 2004; Le Bourdonnec et al., 2010; Mulazzani et al., 2010; Foresta Martin et al., 2017, 2020), as well as from inland BM* and Procida BM* deposits (Fedele et al., 2008).

peralkaline character with both ASI and AI values below 1 (Fig. 10a). In contrast, obsidians from Monte Arci can be barely discriminated based on their peraluminous fingerprint (ASI and AI > 1) by those from Palmarola, which partially overlap in the peraluminous field and extend into the peralkaline field. Lipari obsidians encompass the full compositional range of both Monte Arci and Palmarola sources, spanning from peraluminous to metaluminous and even into peralkaline field. In this diagram, all the BM obsidians plot close to those from Lipari, Palmarola and Monte Arci, falling within both the metalluminous and peraluminous fields, making them difficult to distinguish.

Although not suitable for discriminating purposes, the Shand's diagram is useful to show the compositional variability among the BM and the other Central-Western Mediterranean obsidian sources.

A clear differentiation of the obsidians from the BM compared to those coming from the four Central-Western Mediterranean sources is obtained by using the classification scheme of Peacock (1931), redefined by MacDonald (1992), which is based on the two parameters $SiO_2/(Na_2O + K_2O)$ and CaO content (Fig. 10b). The ratio between silica and alkali of the obsidians found in the different outcrops of the BM is constant (~4.7), and lower than that of the obsidians from the other sources (>5.5); the calcium content varies greatly from 1.4 wt% in the Punta della Lingua obsidian to 3.2 wt% in the inland BM obsidians (Fedele et al., 2008), and is greater than that of the four

main sources of obsidian (<1.2 wt%). However, the other sources, having similar CaO contents, are not clearly distinguishable, except for Pantelleria obsidians which have the lowest $SiO_2/(Na_2O + K_2O)$ ratio (<7).

Foresta Martin et al. (2020) proposed the use of the Na_2O vs. Cl diagram as a tool for distinguishing the provenance of obsidian fragments in archaeological contexts. In this diagram (Fig. 10c), the obsidian from Punta della Lingua BM stands out from all others due to its higher content in Cl (0.7 wt%) at similar Na_2O content to Pantelleria obsidians. Even if with some outliers, Pantelleria obsidians exhibits the highest Cl (up to 0.5 wt%) and Na_2O (~7 wt%) contents, whereas those from Monte Arci display the lowest Cl (~0.1 wt%) and Na_2O (~3.5 wt%) contents. Lipari and Palmarola obsidians have intermediate composition with similar, yet distinguishable, Na_2O (~4.1 wt% and 4.8 wt%, respectively) and Cl (~0.3 wt% and ~0.2 wt%) contents. Therefore, Cl analyses, in conjunction with major elements are extremely useful for the geochemical discrimination of obsidian sources.

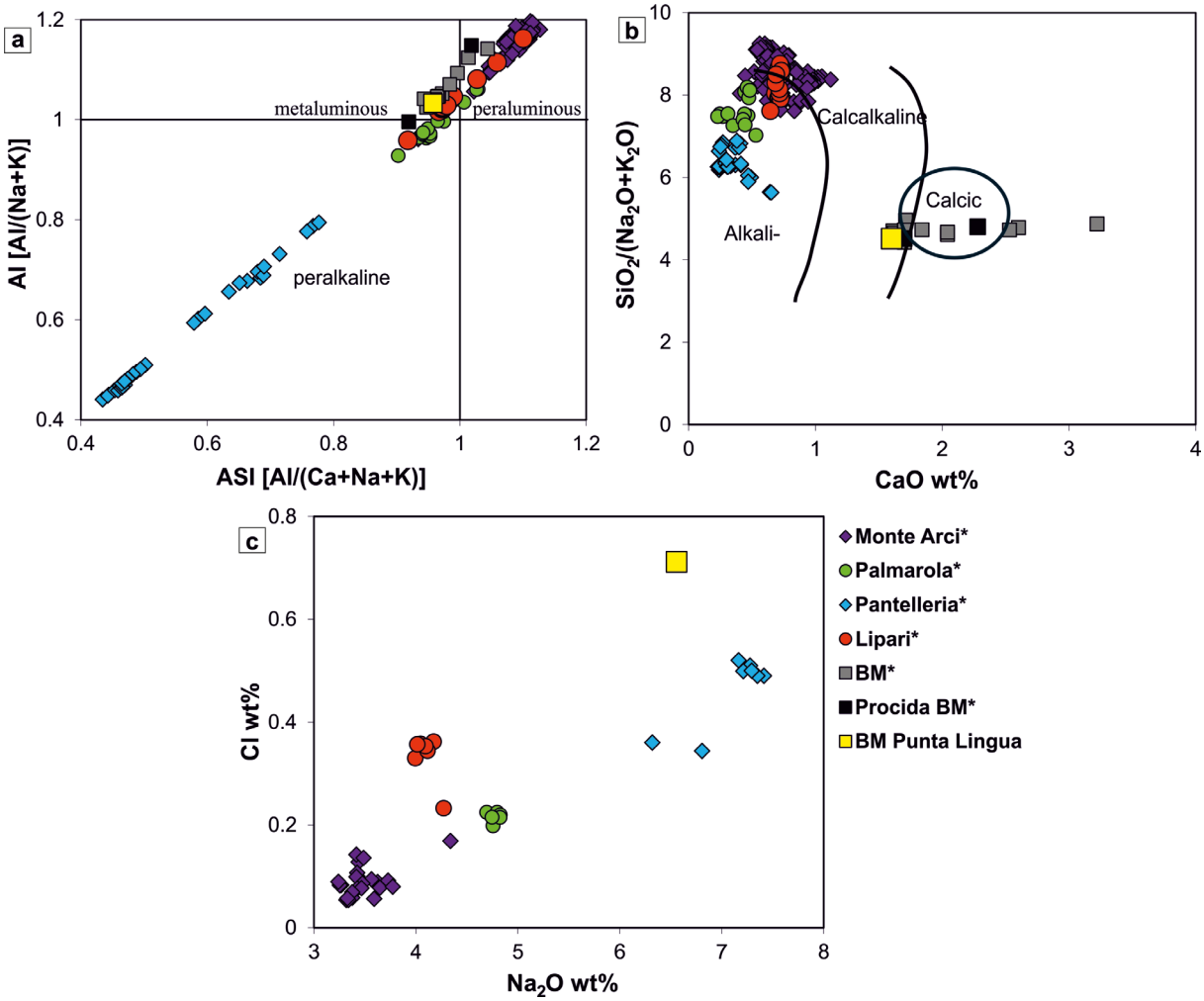

Figure 10. (a) Shand's diagram (Shand, 1927) with the fields redefined by Maniar and Piccoli (1989), (b) CaO (wt%) vs. $SiO_2/(NaO_2 + K_2O)$ diagram (Peacock, 1931; MacDonald, 1992), and (c) Na_2O (wt%) vs. Cl (wt%) diagram showing Punta della Lingua BM obsidian analyzed in this study, compared with literature data of obsidians from Monte Arci*, Palmarola*, Pantelleria*, Lipari* (Francaviglia, 1984, 1988, 1999; Tykot, 2002; Gioncada et al., 2003; Bellot-Gurlet et al., 2004; Le Bourdonnec et al., 2010; Mulazzani et al., 2010; Foresta Martin et al., 2017, 2020), as well as from inland BM* and Procida BM* deposits (Fedele et al., 2008). Clorine data of Monte Arci*, Palmarola*, Pantelleria* and Lipari* obsidians are from Francaviglia (1984), Tykot (2002), Foresta Martin et al. (2017, 2020).

4.3 Isotopic composition of obsidians from Procida, Pantelleria, Palmarola, Lipari and Monte Arci

The Sr and Nd isotopic ratios measured on selected obsidian fragments from the four main prehistoric obsidian sources in the Central-Western Mediterranean and on the BM obsidian fragment from Punta della Lingua are reported in Table 4.

Lipari obsidians are characterized by $^{87}Sr/^{86}Sr$ varying from ~0.70585 to ~0.70597 and roughly constant $^{143}Nd/^{144}Nd$ (~0.5125). Palmarola obsidians have the highest Sr isotopic composition (~0.7135) with $^{143}Nd/^{144}Nd$ of ~0.5123. On the contrary, Pantelleria obsidians are featured by the lowest Sr and the highest Nd isotopic ratios (0.70452-0.70667 and ~0.5129, respectively). Among these extreme values, the obsidians from Monte Arci are characterized by $^{87}Sr/^{86}Sr$ varying from ~0.7078 to ~0.7087 and $^{143}Nd/^{144}Nd$ of ~0.5122. In this frame, the isotopic composition of Punta della Lingua obsidian is intermediate between Lipari and Monte Arci sources (Fig. 11), having Sr isotopic composition ($^{87}Sr/^{86}Sr = 0.7074$) similar to that of Monte Arci and Nd isotopic composition ($^{143}Nd/^{144}Nd = 0.5125$) similar to that of Lipari. Sr and Nd isotopic compositions of the investigated BM obsidian are in the range of values measured on whole rocks, glasses and crystals from the Campanian Ignimbrite evolved magma (e.g., Arienzo et al., 2009).

Even if the Sr isotopic compositions of some of the analyzed obsidians partially overlap, when Sr and Nd isotopic ratios are plotted together the obsidians from the different sources are clearly distinguishable.

This study, together with other recent studies already present in literature (e.g., De Bonis et al., 2018; Di Luzio et al., 2019; Verde et al., 2025) for other archaeological materials, demonstrates that the combined use of the Sr and Nd isotopic compositions of obsidians is highly effective for provenance discrimination.

Table 4. $^{87}Sr/^{86}Sr$ and $^{143}Nd/^{144}Nd$ values measured in obsidians from Punta della Lingua Breccia Museo (BM) in Procida and the main prehistoric obsidian sources in the Central-Western Mediterranean (Lipari, Pantelleria, Palmarola, Monte Arci).

Obsidian source	Locality	Sample	$^{87}Sr/^{86}Sr$	$^{143}Nd/^{144}Nd$
BM (Campanian Ignimbrite)	Punta della Lingua (Procida)	Proc 1	0.707402	0.512502
Lipari	Canneto	Lip Canneto FFM	0.705922	0.512553
	Campo Bianco	Lip Campo Bianco	0.705848	0.512541
	Gabellotto	Lip 1	0.705965	0.512546
		Lip 2	0.705958	0.512525
		Lip 3	0.705973	0.512536
Palmarola	Monte Tramontana	Palm MT	0.71325	0.512339
		Palm 0.1	0.713499	0.512361
		Palm 0.8	0.713785	0.512329
Pantelleria		Pant 0.7	0.706675	0.512939
		Pant 0.8	0.70452	0.512972
Monte Arci		M. Arci SA	0.708779	0.512231
		M. Arci SC	0.70784	0.512323

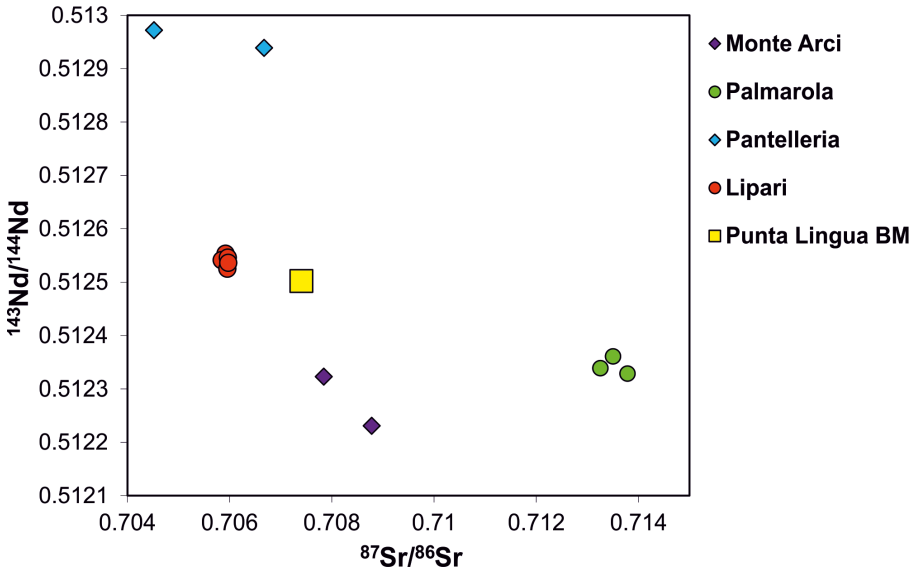

Figure 11. $^{87}Sr/^{86}Sr$ vs. $^{143}Nd/^{144}Nd$ diagram showing the analyzed obsidians from Monte Arci, Palmarola, Pantelleria, Lipari and Punta della Lingua BM.

5. Conclusions

The recent archaeological discovery, on Vivara islet (Procida, Campania region, South Italy), of a prehistoric use of the BM obsidian as abrasive powder, despite previously being considered unsuitable to produce tools or other artifacts of practical use, suggests the need for a more founded/detailed geochemical and petrographic characterization of this volcanic glass associated with the Campanian Ignimbrite eruption occurred about 40 thousand years ago in the Campi Flegrei.

In this study, starting from the characterization of some BM obsidian fragments from Punta della Lingua outcrop on Procida Island, we identify the geochemical "fingerprints" that can be used to discriminate among obsidian fragments found in the same archaeological context, but possibly derived from different geological sources. These fingerprints can be detected through a wide range of analytical techniques, such as SEM-EDS, SEM-WDS, XRF and TIMS.

We compare the BM obsidians, from both Procida and Campi Flegrei inland deposits, with those from the four major Central-Western Mediterranean sources (Lipari, Monte Arci, Pantelleria and Palmarola), which have supplied raw materials to thousands of settlements from the Neolithic to the Bronze Age. Our results highlight the unique morphological and geochemical features of the BM obsidians, clearly distinguishable from all the other sources by their vesicularity, abundance and type of crystals and trachy-phonolitic composition. In particular, the occurrence of a diffuse micro-vesiculation, never observed in other Central-Western Mediterranean obsidian, and the peculiar mineral assemblage, mainly consisting in alkali feldspar, clinopyroxene and plagioclase, can help to distinguish the BM obsidians from the other Central-Western Mediterranean sources even when it is not possible to perform more sophisticated analyses.

Although the morphological analyses and the major elements chemical composition are valuable tools for differentiating the BM obsidians, they prove insufficient for discriminating among all the Central-Western Mediterranean sources. Indeed, the Central-Western Mediterranean sources share similar crystallinity degree and rhyolitic composition with comparable major oxides contents, with the exception of Pantelleria, distinguishable by the presence of amphibole crystals and its higher Fe_2O_{3T} and lower Al_2O_3 contents.

The significant overlap in major element data among Lipari, Palmarola and Monte Arci obsidians highlights the need to consider additional geochemical markers, such as chlorine content and Sr-Nd isotopic ratios. The combination of all these geochemical parameters is essential for an effective differentiation between sources that are otherwise geochemically similar. Notably, when both Sr and Nd isotopes are considered together, no compositional overlap among samples from the studied sources is observed.

Acknowledgements. The activities carried out in the INGV-OV laboratories were supported by the project Pianeta Dinamico-Working Earth (CUP 1466 D53J19000170001 – "Fondo finalizzato al rilancio degli investimenti delle 1467 amministrazioni centrali dello Stato e allo sviluppo del Paese", legge 145/2018) – sub-project SMEEGOL, ref. Ilenia Arienzo.
F.F.M. thanks Profs. Massimiliano Marazzi and Claudio Giardino, and Dr. Federica Bertino for the information regarding the obsidians found during the archaeological excavation at Vivara.
P.D. thanks Mariano Davoli for his assistance during the SEM observation and microanalyses.
The authors are grateful to the reviewers for their valuable suggestions, which strengthened the manuscript.

References

Acquafredda, P. and A. Paglionico (2004). SEM-EDS microanalysis of microphenocrysts of Mediterranean obsidians: a preliminary approach to source discrimination, Eur. J. Mineral., 16, 3, 419-429, doi:10.1127/0935-1221/2004/0016-0419.

Arienzo, I., L. Civetta, A. Heumann, G. Wörner et al. (2009). Isotopic evidence for open system processes within the Campanian Ignimbrite (Campi Flegrei-Italy) magma chamber, Bull. Volcanol., 71, 285-300, doi:10.1007/s00445-008-0223-0.

Arienzo, I., A. Heumann, G. Wörner, L. Civetta et al. (2011). Processes and timescales of magma evolution prior to the Campanian Ignimbrite eruption (Campi Flegrei, Italy), Earth Planet. Sci. Let., 306, 217-228, doi:10.1016/j.epsl.2011.04.002.

Arienzo, I., A. Carandente, V. Di Renzo, P. Belviso et al. (2013). Sr and Nd isotope analysis at the Radiogenic Isotope Laboratory of the Istituto Nazionale di Geofisica e Vulcanologia, Sezione di Napoli – Osservatorio Vesuviano, Rapp. Tec. INGV, 260, ISSN:2039-7941.

Arienzo, I., I. Rucco, M. A. Di Vito, M. D'Antonio et al. (2020). Sr isotopic composition as a tool for unraveling human mobility in the Campania area, Archaeol. Anthropol. Sci., 12, 8, 157, doi:10.1007/s12520-020-01088-0.

Barberi, F., F. Innocenti, L. Lirer, R. Munno et al. (1978). The Campanian Ignimbrite: a major prehistoric eruption in the Neapolitan area (Italy), Bull. Volcanol., 41, 1, 10-31, doi:10.1007/BF02597680.

Bellot-Gurlet, L., F. X. L. Bourdonnec, G. Poupeau and S. Dubernet (2004). Raman micro-spectroscopy of western Mediterranean obsidian glass: one step towards provenance studies?, J. Raman Spectrosc., 35, 8-9, 671-677, doi:10.1002/jrs.1195.

Bertino, F., A. Cazzella, C. Giardino, M. Marazzi et al. (2024). Ossidiana a Vivara. In L'Oro Nero del Mediterraneo, L'ossidiana nella Preistoria. Franco Foresta Martin and Nicola Scotto di Carlo, Villaggio Letterario, Napoli, 190, ISBN:9791280974150.

Cariddi, B., E. Vertechi, A. Caputo, L. Brusca, G. Scarpato et al. (2025). Isotopic measurements of Sr, Nd, Li and Mg standards using the Thermo ScientificTM TritonTM Plus mass spectrometer at the INGV Osservatorio Vesuviano, Rapp. Tec. INGV, 506, 122, doi:10.13127/rpt/506.

Cas, R., J. V. Wright and G. Giordano (2024). Volcanology: Processes, Deposits, Geology and Resources, Springer International Publishing, ISBN:978-3-319-66612-9.

Chataigner, C., J. L. Poidevin and N. O. Arnaud (1998). Turkish occurrences of obsidian and use by prehistoric peoples in the Near East from 14,000 to 6000 BP, J. Volcanol. Geotherm. Res., 85, 1-4, 517-537, doi:10.1016/S0377-0273(98)00069-9.

Civetta, L., G. Orsi, L. Pappalardo, R. V. Fisher et al. (1997). Geochemical zoning, mingling, eruptive dynamics and depositional processes – the Campanian Ignimbrite, Campi Flegrei caldera, Italy, J. Volcanol. Geotherm. Res., 75, 3-4, 183-219, doi:10.1016/S0377-0273(96)00027-3.

D'Antonio, M., I. Arienzo, R. J. Brown, P. Petrosino et al. (2021). Tephrostratigraphic Marker in Distal Sequences of the Central Mediterranean, Minerals, 11, 9, 955, doi:10.3390/min11090955.

De Astis, G., L. Pappalardo and M. Piochi (2004). Procida volcanic history: new insights into the evolution of the Phlegraean Volcanic District (Campania region, Italy), Bull. Volcanol., 66, 7, 622-641, doi:10.1007/s00445-004-0345-y.

De Bonis, A., I. Arienzo, M. D'Antonio, L. Franciosi et al. (2018). Sr-Nd isotopic fingerprinting as a tool for ceramic provenance: Its application on raw materials, ceramic replicas and ancient pottery, J. Archaeolog. Sci., 94, 51-59, doi:10.1016/j.jas.2018.04.002.

Di Girolamo, P., M. R. Ghiara, L. Lirer, R. Munno et al. (1984). Vulcanologia e petrologia dei Campi Flegrei, Boll. Soc. Geol. It., 103, 349-413.

Di Luzio, E., I. Arienzo, S. Boccuti, A. De Meo et al. (2019). Chemical-petrographic and isotopic characterization of the volcanic pavement along the ancient Appia route at the Aurunci Mountain Pass, Italy: Insights on possible provenance, Geoarchaeology, 34, 5, 522-539, doi:10.1002/gea.21718.

Disa, J. J., J. Vossoughi and N. H. Goldberg (1993). A comparison of obsidian and surgical steel scalpel wound healing in rats, Plast. Reconstr. Surg., 92, 5, 884-887, PMID:8415970.

Donato, P., L. Barba, R. De Rosa, G. Niceforo et al. (2018). Green, grey and black: A comparative study of Sierra de las Navajas (Mexico) and Lipari (Italy) obsidians, Quat. Int., 467, 369-390, doi:10.1016/j.quaint.2017.11.021.

Fedele, F. G., B. Giaccio, R. Isaia and G. Orsi (2003). The Campanian Ignimbrite eruption, Heinrich Event 4, and Paleolithic change in Europe: A high-resolution investigation, Geophysical Monograph-American Geophysical Union, 139, 301-328, doi:10.1029/139GM20.

Fedele, L., C. Scarpati, M. Lanphere, L. Melluso et al. (2008). The Breccia Museo formation, Campi Flegrei, southern Italy: geochronology, chemostratigraphy and relationship with the Campanian Ignimbrite eruption, Bull. Volcanol., 70, 10, 1189-1219, doi:10.1007/s00445-008-0197-y.

Fisher, R. V., G. Orsi, M. Ort and G. Heiken (1993). Mobility of a large-volume pyroclastic flow – emplacement of the Campanian ignimbrite, Italy, J. Volcanol. Geotherm. Res., 56, 3, 205-220, doi:10.1016/0377-0273(93)90017-L.

Foresta Martin, F., A. Di Piazza, C. D'oriano, M. L. Carapezza et al. (2017). New insights into the provenance of the obsidian fragments of the island of Ustica (Palermo, Sicily), Archaeometry, 59, 3, 435-454, doi:10.1111/arcm.12270.

Foresta Martin, F. and M. La Monica (2019). The Black Gold that came from the sea. A review of Obsidian studies at the island of Ustica, Ann. Geophys., 62, 1, VO14, doi:10.4401/ag-7686.

Foresta Martin, F., S. G. Rotolo, M. Nazzari and M. L. Carapezza (2020). Chlorine as a discriminant element to establish the provenance of central Mediterranean obsidians, Open Archaeol., 6, 1, 454-476, doi:10.1515/opar-2020-0124.

Francaviglia, V. (1984). Characterization of Mediterranean obsidian sources by classical petrochemical methods, Preistoria Alpina, 20, 311-32.

Francaviglia, V. (1988). Ancient obsidian sources on Pantelleria (Italy), J. Archaeolog. Sci., 15, 2, 109-122.

Francaviglia, V. (1999). The search for a reliable discrimination between Mediterranean obsidians, in Proceedings of Il vetro in Italia meridionale e insulare F. Sogliani and C. Piccioli, 1998, 5-7 March, Napoli, Italy, 315-380.

Fulignati, P., M. Marianelli, M. Proto and A. Sbrana (2004). Evidences for disruption of a crystallizing front in a magma chamber during caldera collapse: an example from the Breccia Museo unit (Campanian Ignimbrite eruption, Italy), J. Volcanol. Geotherm. Res., 133, 141-155, doi:10.1016/S0377-0273(03)00395-0.

Giaccio, B., E. M. Niespolo, A. Pereira, S. Nomade et al. (2017). First integrated tephrochronological record for the last ~190 kyr from the Fucino Quaternary lacustrine succession, central Italy, Quat. Sci. Rev., 158, 211-234, doi:10.1016/j.quascirev.2017.01.004.

Gioncada, A., R. Mazzuoli, M. Bisson and M. T. Pareschi (2003). Petrology of volcanic products younger than 42 ka on the Lipari-Vulcano complex (Aeolian Islands, Italy): an example of volcanism controlled by tectonics, J. Volcanol. Geotherm. Res., 122, 3-4, 191-220, doi:10.1016/S0377-0273(02)00502-4.

Goldstein, S. L., P. Deines, E. H. Oelkers, R. L. Rudnick et al. (2003). Standards for publication of isotope ratio and chemical data in Chemical Geology, Chem. Geol., 202, 1-4, doi:10.1016/j.chemgeo.2003.08.003.

Johnston-Lavis, H. J. (1888). Excavation near Naples. Report of the Committee Appointed for the Investigation of the Volcanic Phenomena of Vesuvius and its Neighbourhood, Spottiswoode and Co., London, 1-7.

Le Bas, M. J., R. W. Le Maitre, A. Streckeisen and B. Zanettin (1986). A chemical classification of volcanic rocks based on the total alkali-silica diagram, J. Petrol., 27, 745-750, doi:10.1093/petrology/27.3.745.

Le Bourdonnec, F. X., J. M. Bontempi, N. Marini, S. Mazet et al. (2010). SEM-EDS characterization of western Mediterranean obsidians and the Neolithic site of A Fuata (Corsica), J. Archaeol. Sci., 37, 1, 92-106, doi:10.1016/j.jas.2009.09.016.

Lirer, L., G. Rolandi and M. Rubin (1991). ^{14}C Age of the "Museum Breccia" (Campi Flegrei) and its relevance for the origin of the Campanian Ignimbrite, J. Volcanol. Geotherm. Res., 48, 223-227, doi:10.1016/0377-0273(91)90044-Z.

Macdonald, R., R. L. Smith and J. E. Thomas (1992). Chemistry of the subalkalic silicic obsidians, U. S. Geological Survey, 1523, 214, doi:10.3133/pp1523.

Maniar, P. D. and P. M. Piccoli (1989). Tectonic discrimination of granitoids, Geol. Soc. Am. Bull., 101, 5, 635-643, doi:10.1130/0016-7606(1989)1012.3.CO;2.

Marazzi, M. and S. Tusa (1994). Vivara, centro commerciale mediterraneo dell'età del Bronzo, II: le tracce dei contatti con il mondo egeo (scavi 1976-1982), Bagatto Libri, Roma, ISBN:8878060844.

Melluso, L., V. Morra, A. Perrotta, C. Scarpati et al. (1995). The eruption of the Breccia Museo (Campi Flegrei, Italy): Fractional crystallization processes in a shallow, zoned magma chamber and implications for the eruptive dynamics, J. Volcanol. Geotherm. Res., 68, 325-339, doi:10.1016/0377-0273(95)00020-5.

Mulazzani, S., F. X. Le Bourdonnec, L. Belhouchet, G. Poupeau et al. (2010). Obsidian from the Epipalaeolithic and Neolithic eastern Maghreb. A view from the Hergla context (Tunisia), J. Archaeol. Sci., 37, 10, 2529-2537, doi:10.1016/j.jas.2010.05.013.

Orsi, G., S. de Vita and M. A. di Vito (1996). The restless, resurgent Campi Flegrei nested caldera (Italy): constraints on its evolution and configuration, J. Volcanol. Geotherm. Res., 74, 179-214, doi:10.1016/S0377-0273(96)00063-7.

Pappalardo, L., L. Civetta, S. de Vita, M. A. Di Vito et al. (2002). Timing of magma extraction during the Campanian Ignimbrite eruption (Campi Flegrei Caldera), J. Volcanol. Geotherm. Res., 114, 479-497, doi:10.1016/S0377-0273(01)00302-X.

Pasquetti, F., G. Zanchetta, M. Bini, J. Paffi et al. (2023). Potential dust sources for loess deposits in Central Italy: A geochemical case study from the Loess-Paleosol-Sequence of Ponte Crispiero (Marche), Catena, 226, 107064, doi:10.1016/j.catena.2023.107064.

Peacock, M. A. (1931). Classification of igneous rock series, J. Geol., 39, 1, 54-67.

Perrotta, A. and C. Scarpati (1994). The dynamics of the Breccia Museo eruption (Campi Flegrei, Italy) and the significance of spatter clasts associated with lithic breccias, J. Volcanol. Geotherm. Res., 59, 335-355, doi:10.1016/0377-0273(94)90086-8.

Perrotta, A., C. Scarpati, G. Luongo and V. Morra (2006). Chapter 5 The Campi Flegrei caldera boundary in the city of Naples, Dev. Volcanol., 9, 85-96, doi:10.1016/S1871-644X(06)80019-7.

Petrosino, P., I. Arienzo, F. C. Mazzeo, J. Natale et al. (2019). The San Gregorio Magno lacustrine basin (Campania, southern Italy): improved characterization of the tephrostratigraphic markers based on trace elements and isotopic data, J. Quat. Sci., 34, 6, 393-404, doi:10.1002/jqs.3107.

Pyle, D. M. (2015). Chapter 13 – Sizes of volcanic eruptions, The encyclopedia of volcanoes, 257-264, doi:10.1016/B978-0-12-385938-9.00013-4.

Pyle, D. M., G. D. Ricketts, V. Margari, T. H. van Andel et al. (2006). Wide dispersal and deposition of distal tephra during the Pleistocene 'Campanian Ignimbrite/Y5' eruption, Italy, Quat. Sci. Rev., 25, 2713-2728, doi:10.1016/j.quascirev.2006.06.008.

Rittmann, A. (1950). Sintesi geologica dei Campi Flegrei, Boll. Soc. Geol. Ital., 69, 117-128.

Romboni, M., I. Arienzo, M. A. Di Vito, C. Lubritto et al. (2023). La Sassa cave: isotopic evidence for Copper Age and Bronze Age population dynamics in Central Italy, PLoS One, 18, 7, e0288637, doi:10.1371/journal.pone.0288637.

Rosi, M., L. Vezzoli, P. Aleotti and M. De Censi (1996). Interaction between caldera collapse and eruptive dynamics during the Campanian Ignimbrite eruption, Phlegrean Fields, Italy, Bull. Volcanol., 57, 541-554, doi:10.1007/BF00304438.

Rosi, M., L. Vezzoli, A. Castelmenzano and G. Greco (1999). Plinian pomice fall deposit of the Campanian Ignimbrite eruption (Phlegrean Fields Italy), J. Volcanol. Geotherm. Res., 91, 179-198, doi:10.1016/S0377-0273(99)00035-9.

Rotolo, S. G., M. L. Carapezza, A. Correale, F. F. Martin et al. (2020). Obsidians of Pantelleria (Strait of Sicily): A petrographic, geochemical and magnetic study of known and new geological sources, Open Archaeol., 6, 1, 434-453, doi:10.1515/opar-2020-0120.

Scott, M. J. and M. J. Scott (1982). Obsidian Surgical Blades: Modern Use of a Stone Age Implement, Dermatol. Surg., 8, 1050-1052, doi:10.1111/j.1524-4725.1982.tb01093.x.

Shand, S. J. (1927). Eruptive rocks: their genesis, composition, classification, and their relation to ore-deposits, with a chapter on meteorites, T. Murby & Company.

Silleni, A., G. Giordano, R. Isaia and M. H. Ort (2020). The Magnitude of the 39.8 ka Campanian Ignimbrite Eruption, Italy: Method, Uncertainties and Errors, Front. Earth Sci., 8, 543399, doi:10.3389/feart.2020.543399.

Sparice, D., C. Pelullo, S. de Vita, I. Arienzo et al. (2024). The pre-Campi Flegrei caldera (>40 ka) explosive volcanic record in the Neapolitan Volcanic Area: New insights from a scientific drilling north of Naples, southern Italy, J. Volcanol. Geotherm. Res., 455, 108209, doi:10.1016/j.jvolgeores.2024.108209.

Trasatti, E., C. Magri, V. Acocella, C. Del Gaudio et al. (2023). Magma transfer at Campi Flegrei caldera (Italy) after the 1538 AD eruption, Geophys. Res. Lett., 50, 11, e2022GL102437, doi:10.1029/2022GL102437.

Tykot, R. H. (2002). Chemical fingerprinting and source tracing of obsidian: the central Mediterranean trade in black gold, Acc. Chem. Res., 35, 8, 618-627, doi:10.1021/ar000208p.

Tykot, R. H. (2021). Obsidian in Prehistory, in Encyclopedia of Glass Science, Technology, History and Culture P. Richet, R. Conradt, A. Takada and J. Dyon (Eds.), doi:10.1002/9781118801017.ch10.1.

Verde, M., A. De Bonis, M. D'Antonio, V. Renson et al. (2025). Unveiling the distinctive geochemical signature of fine ware through Sr-Nd-Pb isotopes: A site-specific perspective from the site of Cales (South Italy), Geoarchaeology, 40, e22021, doi:10.1002/gea.22021.

Williams-Thorpe, O. (1995). Obsidian in the Mediterranean and the Near East: A provenancing success story, Archaeometry, 37, 2, 217-248, doi:10.1111/j.1475-4754.1995.tb00740.x.

Zhang, W. and Z. Hu (2020). Estimation of isotopic reference values for pure materials and geological reference materials, At. Spectrosc., 41, 93-102, doi:10.46770/AS.2020.03.001.

***CORRESPONDING AUTHOR: Bruna CARIDDI**,
Istituto Nazionale di Geofisica e Vulcanologia (INGV), Sezione Osservatorio Vesuviano, Naples, Italy
e-mail: bruna.cariddi@ingv.it